DiRong1.0: a distributed implementation for improving routing network generation in model coupling

Hao Yu[1], Li Liu[1], Chao Sun[1], Ruizhe Li[1], Xinzhu Yu[1], Cheng Zhang[1], Zhiyuan Zhang[2], Bin Wang[1,3]

[1] Ministry of Education Key Laboratory for Earth System Modeling, Department of Earth System Science, Tsinghua University, Beijing, China

[2] Hydro-Meteorological Center of Navy China, Beijing China

[3] State Key Laboratory of Numerical Modeling for Atmospheric Sciences and Geophysical Fluid Dynamics (LASG), Institute of Atmospheric Physics, Chinese Academy of Sciences, Beijing, China

Correspondence to: Li Liu (liuli-cess@tsinghua.edu.cn)

Abstract. It is a fundamental functionality of a coupler for Earth system modeling to efficiently handle data transfer between component models. As an approach of *MxN* communication following a routing network has been used in existing couplers for achieving data transfer, routing network generation is generally a major step for initializing the *MxN* communication. Some existing couplers such as MCT and C-Coupler employ an inefficient global implementation for routing network generation that relies on gather/broadcast communications. That's an important reason why the initialization cost of a coupler increases when using more processor cores. In this paper, we propose a **D**istributed **i**mplementation for **Ro**uting **n**etwork **g**eneration, version 1.0 (DiRong1.0), which does not introduce any gather/broadcast communication. The empirical evaluations show that DiRong1.0 is much more efficient than the global implementation. DiRong1.0 has already been implemented in C-Coupler2. We believe that some other couplers can also benefit from it.

1 Introduction

A coupled model regarding Earth system Modelling and numerical weather forecasting generally highly depends on existing couplers (Hill et al., 2004; Craig et al., 2005; Larson et al., 2005; Balaji et al., 2006; Redler et al., 2010; Craig et al., 2012; Valcke, 2013; Liu et al., 2014; Hanke et al., 2016; Craig et al., 2017; Liu et al., 2018), each of which can combine different component models into a whole system and handle data interpolation between different model grids and data transfer between component models (Valcke, 2012).

The functionality of data interpolation generally takes two major steps, i.e., preparing remapping weights that are from an offline file or from online calculation when initializing the coupler, and conducting parallel interpolation calculation based on the sparse matrix-vector multiplication with the remapping weights throughout the coupled model integration. The functionality of data transfer of couplers is transferring scalar variables or fields on a model grid (called gridded fields hereafter) from one component model to another via MPI (Message Passing Interface). A component model generally has been parallelized through decomposing the cells of a model grid into distinct subsets each of is assigned to an MPI process for cooperative concurrent computation, e.g., the sample parallel decompositions in Fig. 1a and 1b. To efficiently transfer gridded fields in parallel, Jacob et al. (2005) proposed an approach of *MxN* communication (called *MxN* approach) following a routing network where each pair of processes from the two component models should have a communication connection only when they have common grid cells (for example, Fig. 1c). This *MxN* approach has already been used in existing couplers for more than ten years. As the parallel decompositions of component models generally keep constant throughout the whole integration, a routing network can also keep constant. Thus, the *MxN* approach can be achieved with two major steps: generating the routing network when initializing the coupler, and transferring gridded fields based on the routing network throughout the coupled model integration.

In response to more and more computation resulting from higher and higher resolutions in model development, the parallel efficiency of a coupled model on modern high-performance computers becomes more and more critical. Any module in a coupled model, including the coupler, can impact the parallel efficiency of the whole coupled model. Most existing couplers achieve scalable data transfer and data interpolation throughout the coupled model integration, i.e., the data transfer and data interpolation generally can be faster when using more processor cores, while experiences from OASIS3-MCT and C-Coupler2 have shown that the initialization cost of a coupler can increase rapidly when using more processor cores (Craig et al., 2017; Liu et al., 2018). A further investigation in Fig. 2 based on MCT shows that the initialization of data transfer, i.e., generating routing networks, is an important source of the initialization cost.

To lower the initialization cost of a coupler, this paper tries to make a first step through focusing on the generation of routing networks, and proposes a new **D**istributed **i**mplementation for **Ro**uting **n**etwork **g**eneration, version 1.0 (DiRong1.0). The evaluation based on C-Coupler2 shows that, it is much faster than the existing approach. The remainder of this paper is organized as follows. We investigate the existing implementations in Section 2, present and then evaluate DiRong1.0 in Section 3 and 4 respectively, and conclude and discuss this work in Section 5.

2 Existing implementations of routing network generation

In some couplers such as MCT and C-Coupler, the global information of a parallel decomposition is originally distributed among all processes of a component model, where a process only records its local parallel decomposition corresponding to the grid cells assigned to it. Thus, these couplers generally use the following 4 steps for generating a routing network between the parallel decompositions of a source (*src*) and a destination (*dst*) component model.

1) Gathering global parallel decomposition: the *src*/*dst* root process gathers the global information of the *src*/*dst* parallel decomposition from all *src*/*dst* processes.
2) Exchanging global parallel decomposition: the *src*/*dst* root process first exchanges the *src*/*dst* global parallel decomposition with the *dst*/*src* root process, and then broadcasts the *dst*/*src* global parallel decomposition to all *src*/*dst* processes.
3) Detecting common grid cells: each *src*/*dst* process detects its common grid cells with each *dst*/*src* process based on its local parallel decomposition and the *dst*/*src* global parallel decomposition.
4) Generating the routing network: each *src*/*dst* process generates its local routing network according to the information about common grid cells.

Given that each of the *src* and *dst* component models uses *K* processes and the corresponding grid size is *N* (the grid has *N* cells), the first and second steps correspond to gather/broadcast communications with the time complexity of at least $O(N*logK)$ and the memory complexity of $O(N)$. Regarding the third step, the average time complexity corresponding to MCT (as well as CPL6/CPL7 and OASIS3-MCT that employ MCT for data transfer) on each *src*/*dst* process can be $O(N*N/K)$, because the main loop of this step consists of two levels, i.e., the first level corresponds to the local parallel decomposition (the average number of cells in the local parallel decomposition is N/K) while the second level corresponds to the *dst*/*src* global parallel decomposition. The average time complexity of the third step corresponding to C-Coupler is $O(N)$, as C-Coupler first generates a map corresponding to the global parallel decomposition and next detects common cells based on looking up the map. Although this implementation can lower the time complexity, but introduces inefficient irregular memory accesses. As the last step does not depend on any global parallel decomposition, its average time complexity is $O(N/K)$.

Determined by the gather/broadcast communications (the first and second steps) and the corresponding time complexity of $O(N*logK)$, and the time complexity of $O(N*N/K)$ or $O(N)$ corresponding to common grid cells detection (the third step), such existing implementations of routing network generation are of course inefficient under the increment of processor cores. Moreover, in response to the memory complexity of $O(N)$, more memory will be consumed with finer model grids.

In the following context, the existing implementations relying on gather/broadcast communications are called global routing network generation.

3 Design and implementation

3.1 Overall design

The design and implementation of DiRong1.0 significantly benefits the generally idea of distributed directory (Pinar and Hendrickson, 2001) that has already been used in coupler development (Theurich et al, 2008, Hanke et al., 2016), and different kinds of specific distributed directories are defined and used in DiRong1.0.

To generate the *MxN* data transfer, each cell of a grid can be numbered with a unique index from 1 to *N* (called global cell index), while each grid cell assigned to the same process can also be numbered with a unique local cell index. Thus, the information of a given parallel decomposition can be recorded as a Cell Local-Global Mapping Table (CLGMT), each element of which is a triple of global cell index, process ID, and local cell index. For example, Tables 1 and 2 are the CLGMTs corresponding to the parallel decompositions in Fig. 1a and Fig. 1b respectively.

Generally, the CLGMT entries of a parallel decomposition are distributed among the processes of a component model, which means a process only stores a part of the CLGMT. The key idea of the existing global implementation can be summarized as reconstructing the global CLGMT of the peer parallel decomposition in each process for routing network generation. To be an efficient solution, DiRong1.0 should be fully based on distributed CLGMT without reconstructing any global CLGMT. The reason why the existing global implementations have to depend on global CLGMTs is because the distribution of the CLGMT entries is determined by a model and thus a coupler generally has to view any distribution as random.

Motivated by the above analysis, the key challenge to DiRong1.0 becomes how to efficiently rearrange the original distribution of the CLGMT entries of a given parallel decomposition into a regular intermediate distribution and how to efficiently generate the routing network based on the intermediate distribution. Specifically, we employ a regular intermediate distribution that evenly distributes the CLGMT entries among processes based on the ascending order of the global cell index. Such an intermediate distribution is not only simple, but also enables to easily achieve the rearrangement to the intermediate distribution via a sorting procedure similar to distributed sort. With the above preparations, DiRong1.0 is designed with the following major steps for generating a routing network between the *src* and *dst* component models:

1) The *src*/*dst* component model rearranges the original distribution of the CLGMT entries of the *src*/*dst* parallel decomposition into the regular intermediate distribution.
2) The *src* and *dst* component models exchange the CLGMT entries based on the intermediate distributions.
3) Each *src*/*dst* process generates table entries of the sharing relationship about how each grid cell is shared between the processes of the *src* and *dst* component models, based on the *src* and *dst* CLGMT entries on the intermediate distributions.

4) The *src*/*dst* component model rearranges the intermediate distribution of the entries of the sharing relationship table (SRT) into the original distribution of the CLGMT entries of the *src*/*dst* parallel decomposition.
5) Each *src*/*dst* process generates its local routing network based on the local SRT entries.

In the following context of this section, we will detail the implementation of each major step except the last one because it is similar to the last major step in the global implementation.

3.2 Rearranging CLGMT entries intra a component model

Such rearrangement is achieved via a divide-and-conquer sorting procedure that is similar to a merge sort with the keyword of global cell index. This procedure first sorts the CLGMT entries locally in each process, and next iteratively conducts distributed sort by a main loop of *logK* iterations (*K* is the number of processes of the *src*/*dst* component model). In an iteration, processes are divided into distinct pairs and the two processes in each pair swap the CLGMT entries based on a point-to-point communication. Figure 3 shows an example of the distributed sort corresponding to the CLGMT entries in Table 1, and Table 3 shows the distributed CLGMT after rearranging the CLGMT entries in Table 2. As shown in Fig. 3, the distributed sort employed in DiRong1.0 uses a similar butterfly communication pattern as various optimized collective communication operations and an optimized matrix-vector multiplication (Brooks, 1986; Hendrickson et al, 1995; Thakur et al., 2005).

3.3 Exchanging CLGMT entries between component models

After the rearrangement of the CLGMT in a component model, the CLGMT entries are sorted in an ascending order of the global cell indexes and evenly distributed among processes. The CLGMT entries reserved in each process therefore have a determinate and non-overlapping range of global cell indexes, and such a range can be easily calculated from the grid size, the number of total processes, and process ID. Thus, it is easy to calculate the overlapping relationship of global cell index range between a *src* process and a *dst* process. As it is only necessary to exchange CLGMT entries between a pair of *src* and *dst* processes with overlapping ranges, point-to-point communications only are enough for handling the exchange of the CLGMT entries.

3.4 Generation of SRT

After the previous major step, each process reserves two sequences of CLGMT entries corresponding to the *src* and *dst* parallel decompositions respectively. Given that the two sequences contain *n1* and *n2* entries respectively, the time complexity of detecting the sharing relationship is *O*(*n1*+*n2*), because the entries in each sequence have already been ordered in ascending global cell indexes, and a procedure similar to the kernel of merge sort that merges two ordered data sequences can handle such detection.

To record the sharing relationship, a SRT entry is designed as a quintuple of global cell index, *src* process ID, *src* local cell index, *dst* process ID, and *dst* local cell index. Given a quintuple <q_1,q_2,q_3,q_4,q_5>, it means that number q_3 local cell in number q_2 process of the *src* component model is number q_1 global cell, and the data on it will be transferred to number q_5 local cell in number q_4 process of the *dst* component model. Table 4 shows the SRT in the *src* component model, calculated from the rearranged distributed CLGMT entries in Fig. 3 and Table 3.

It is possible that multiple *src* CLGMT entries correspond to the same global cell index. Under such a case, any *src* CLGMT entry can be used for generating the corresponding SRT entries, because the *src* component model should guarantee that the data copies on the same grid cell are exactly the same. Given a *dst* CLGMT entry, if there is no *src* CLGMT entry with the same global cell index, no SRT entry will be generated. Given that multiple *dst* CLGMT entries correspond to the same global cell index and there is at least one *src* CLGMT entry with the same global cell index, a SRT entry will be generated for each *dst* CLGMT entry.

3.5 Rearranging SRT entries intra a component model

After the previous major step, the SRT entries are distributed among processes of a component model according to the intermediate distribution. As a process can use only the SRT entries corresponding to its local cells for the last major step of local routing network generation, the SRT entries should be rearranged among the processes of a component model. We find that such rearrangement can also be achieved via a sorting procedure similar to the distributed sort with the keyword of *src*/*dst* process ID, or even the sorting procedure implemented for the first major step can be reused. Tables 5 and 6 show the SRT entries distributed in the *src* and *dst* component model respectively, after the rearrangement.

3.6 Time complexity and memory complexity

As DiRong1.0 does not reconstruct the global CLGMT, it does not rely on any gather/broadcast communication, and its average memory complexity is $O(N/K)$ on each process. As the implementation of its most time-consuming major steps are similar to a merge sort, and the time complexity of merge sort is $O(N*logN)$, the average time complexity of DiRong1.0 on each process is $O(N*(logN)/K)$, and average communication complexity is $O(N*(logK)/K)$.

To facilitate the implementation of the sorting procedure, we force the number of processes regarding the 1st ~ 4th major steps (Section 3.1) to be the maximum power of 2 (2^n) no larger than the total process number of the *src*/*dst* component model. For a process whose ID *I* is not smaller than 2^n, its CLGMT entries will be merged into the process with the ID of $I\text{-}2^n$ before the first major step, and the SRT entries corresponding to it will be obtained from the process with the ID of $I\text{-}2^n$ after the fourth major step. This strategy will not change the above time complexity and memory complexity of DiRong1.0, as 2^n is larger than a half of the total process number.

4 Evaluation

For evaluating DiRong1.0, we implemented it in C-Coupler2, which enables us to compare it with the original global routing network generation in C-Coupler2. We developed a toy coupled model consisting of two toy component models and C-Coupler2 for the evaluation, which enables us to flexibly change the model settings in terms of grid size and number of processor cores (processes). The toy coupled model is run on a supercomputer, where each computing node on the supercomputer includes two Intel Xeon E5-2678 v3 CPUs (Intel(R) Xeon(R) CPU (24 processor cores in total)), and all computing nodes were connected with an InfiniBand network. The codes were compiled by an Intel Fortran and C++ compiler at the optimization level O2, using an Intel MPI library (2018 Update 2). A maximum number of 3200 cores are used for running the toy coupled model. All test results are from the average of multiple runs of the toy coupled model.

We made an evaluation under the variation of process numbers (Fig. 4; two component models use the same number of processor cores). For the grid size of 500,000 (Fig. 4a), the execution time of DiRong1.0 does not really decrease when using more processor cores. This result is reasonable although it does not match the time complexity of DiRong1.0. The communication complexity of DiRong1.0 is $O(N*(logK)/K)$, where *logK* stands for the number of point-to-point communications in each process and *N*/*K* stands for the average message size in each communication. The average message size corresponding Fig. 4a is small (about 160KB under 60 cores while about 6KB under 1600 cores for each toy component model), while the execution time of point-to-point communication cannot keep linear to the message size and may be unstable when the message size is small. Different from DiRong1.0, the execution time of the global implementation increases rapidly with the increment of core number. As a result, DiRong1.0 outperforms the global implementation more significantly when using more cores. When the grid size gets larger (e.g., 4,000,000 in Fig. 4b and 16,000,000 in Fig. 4c), DiRong1.0 still significantly outperforms the global implementation, while with better scalability.

Considering a model can use more processor cores for acceleration when its resolution gets finer, we further evaluated the weak scalability of DiRong1.0, where we concurrently increased the grid size and core number to achieve similar numbers of grid points per process. As shown in Table 7, the execution time of DiRong1.0 increases slowly while the execution time of the global implementation increases rapidly with the increment of grid size and core number. This demonstrates that DiRong1.0 achieves much better weak scalability than the global implementation.

5 Conclusion and discussion

In this paper, we propose a new distributed implementation, DiRong1.0, for routing network generation. As it does not introduce any gather/broadcast communication and achieves much lower complexity in terms of time, memory and communication than the global implementation, it is of course much more efficient than the global implementation. The evaluation results further demonstrate this conclusion. DiRong1.0 has already been implemented in C-Coupler2. Its code is publicly available in a C-Coupler2 version and will be further used in future C-Coupler versions. We do believe that some existing couplers such as MCT, OASIS3-MCT and CPL6/CPL7, can also benefit from DiRong1.0, for accelerating the routing network generation as well as the coupler initialization.

We did not evaluate the impact of DiRong1.0 on the total time of a model simulation, because this impact can be relative. The overhead of routing network generation as well as coupler initialization will be trivial under a long simulation (e.g., hundreds of model days or even hundreds of model years), but may be significant for a short simulation (e.g., several model days or even several model hours in weather forecasting (Palmer et al., 2008; Hoskins, 2013)). In a data assimilation for weather forecasting, it can be required to start a model run just for only several model hours or even shorter. Regarding an operational model, there is generally a time limitation of producing forecasting results (for example, finishing 5-day forecasting in two hours), and thus developers always have to carefully optimize various software modules especially when the model resolution gets finer. In fact, we have been asked to accelerate the initialization of C-Coupler2 for an operational coupled model used in China, and that’s a main reason why we developed DiRong1.0.

Another main reason why we developed DiRong1.0 is that, routing network generation will become more important along with the development of C-Coupler. Recently, a new framework for weakly coupled **e**nsemble **d**ata **a**ssimilation (EDA) based on C-Coupler2, named DAFCC1 (Sun et al., 2020), was developed. DAFCC1 will be an important part in C-Coupler3, the next version of C-Coupler. Given a coupled EDA system and that users want the atmosphere component to perform EDA, DAFCC1 will automatically generate an ensemble component corresponding to all ensemble members of the atmosphere component for calling the DA algorithm, and will automatically conduct routing network generation for the data transfers between the ensemble component and each ensemble member. Thus, routing network generation will be more frequently used in EDA with DAFCC1. For example, given that there are 50 ensemble members, the routing network generation with the ensemble component will be conducted at least 50 times.

We note that, the current sequential read of a remapping weight file is another bottleneck of C-Coupler2. Similar to Hanke et al. (2016), we will design a specific distributed directory for reading in the remapping weights in parallel, while will enable to efficiently redistribute remapping weights among processes based on DiRong1.0. Currently, C-Coupler2 employs a simple global representation for horizontal grids, which means that each process keeps all points of a horizontal grid. The global representation will become a bottleneck in at least two aspects. First, it will consume too much memory to run a model simulation. For example, given a horizontal grid with 16,000,000 points, the memory for keeping it in each process will be about 1.3GB (given that each point has four vertexes and the data type is double precision), which is a large memory requirement. Second, initialization of the data interpolation functionality requires exchanging model grids between different component models, which introduces global communications (e.g., broadcast) for the global grid representations. To address this bottleneck, we will design and develop a distributed grid representation that can be viewed as a specific distributed directory, will enable to efficiently redistribute horizontal grid points among processes based on DiRong1.0.

Code availability. The source code of DiRong1.0 can be viewed and run with C-Coupler2 and the toy coupled model via https://doi.org/10.5281/zenodo.3971829. The MCT version corresponding to Fig. 2 is 2.10 (https://www.mcs.anl.gov/research/projects/mct/).

Author contributions. HY was responsible for code development, software testing and experimental evaluation of DiRong1.0, and co-led paper writing. LL initiated this research, was responsible for the motivation and design of DiRong1.0, supervised HY, and co-led paper writing. CS, RL, XY and CZ contributed to code development and software testing. ZZ and BW contributed to the motivation and software testing. All authors contributed to improvement of ideas and paper writing.

Competing interests. The authors declare that they have no conflict of interest.

Acknowledgements. This work was jointly supported in part by the National Key Research Project of China (grant no. 2017YFC1501903).

References

Balaji, V., J. Anderson, I. Held, M. Winton, J. Durachta, S. Malyshev, and R. J. Stouffer, 2006: The Exchange Grid: a mechanism for data exchange between Earth System components on independent grids. In: Proceedings of the 2005 International Conference on Parallel Computational Fluid Dynamics, College Park, MD, USA, Elsevier, 2006.

E. D. Brooks,1986: The Butterfly Barrier. International Journal of Parallel Programming,15(4):295–307

Craig, A. P., M. Vertenstein, and R. Jacob, 2012: A New Flexible Coupler for Earth System Modelling developed for CCSM4 and CESM1. Int. J. High Perform. C, 26-1, 31–42, doi:10.1177/1094342011428141.

Craig, A. P., R. L. Jacob, B. Kauffman, T. Bettge, J. W. Larson, E. T. Ong, C. H. Q. Ding, Y. He, 2005: CPL6: The New Extensible, High Performance Parallel Coupler for the Community Climate System Model. International Journal of High Performance Computing Applications, 19(3): 309-327.

Craig, A., Valcke, S., and Coquart, L.: Development and performance of a new version of the OASIS coupler, OASIS3-MCT_3.0, Geosci. Model Dev., 10, 3297-3308, https://doi.org/10.5194/gmd-10-3297-2017, 2017

Hanke, M., Redler, R., Holfeld, T., and Yastremsky, M.: YAC 1.2.0: new aspects for coupling software in Earth system modelling, Geosci. Model Dev., 9, 2755–2769, https://doi.org/10.5194/gmd-9-2755-2016, 2016

Hendrickson, B., R. Leland, and S. Plimpton. An efficient parallel algorithm for matrix-vector multiplication. International Journal of High Speed Computing 7, no. 01(1995): 73-88.

Hill, C., C. DeLuca, V. Balaji, M. Suarez, and A. da Silva, 2004: Architecture of the Earth System Modelling Framework. Comput. Sci. Eng., 6, 18–28.

Hoskins, B.: The potential for skill across the range of the seamless weather-climate prediction problem: a stimulus for our science, Q. J. Roy. Meteor. Soc., 139, 573-584, 2013.

Jacob, R., J. Larson, and E. Ong, 2005: M x N Communication and Parallel Interpolation in Community Climate System Model Version 3 Using the Model Coupling Toolkit, Int. J. High. Perform. C, 19, 293–307.

Larson, J., R. Jacob, and E. Ong, 2005: The Model Coupling Toolkit: A New Fortran90 Toolkit for Building Multiphysics Parallel Coupled Models. Int. J. High Perform, C, 19, 277–292.

Liu, L., Yang, G., Wang, B., Zhang, C., Li, R., Zhang, Z., Ji, Y., and Wang, L.: C-Coupler1: a Chinese community coupler for Earth system modeling, Geosci. Model Dev., 7, 2281-2302, doi:10.5194/gmd-7-2281-2014, 2014.

Liu, L., Zhang, C., Li, R., Wang, B., and Yang, G.: C-Coupler2: a flexible and user-friendly community coupler for model coupling and nesting, Geosci. Model Dev., 11, 3557-3586, https://doi.org/10.5194/gmd-11-3557-2018, 2018.

Palmer, T. N., Doblas-Reyes, F. J., Weisheimer, A. and Rodwell, M. J.: Toward seamless prediction: Calibration of climate change projections using seasonal forecasts, Bull. Am. Meteorol. Soc., 89, 459-470, 2008.

Pinar, A. and Hendrickson, B.: Communication Support for Adaptive Computation, Proceedings of the Tenth SIAM Conference on Parallel Processing for Scientific Computing, Portsmouth, Virginia, USA, 12–14 March 2001, SIAM, 2001

R. Redler, S. Valcke and H. Ritzdorf. OASIS4 - a coupling software for next generation earth system modeling. Geosci. Model Dev., 2010, 3(1): 87~104.

Sun, C., Liu, L., Li, R., Yu, X., Yu, H., Zhao, B., Wang, G., Liu, J., Qiao, F., and Wang, B.: Developing a common, flexible and efficient framework for weakly coupled ensemble data assimilation based on C-Coupler2.0, Geosci. Model Dev. Discuss., https://doi.org/10.5194/gmd-2020-75, in review, 2020.

Thakur, R., Rabenseifner, R., Gropp, W. (2005). Optimization of Collective Communication Operations in MPICH. The International Journal of High Performance Computing Applications, 19(1), 49–66. https://doi.org/10.1177/1094342005051521

G. Theurich, ESMF Core Team: Performance Optimization of ESMF. https://www.earthsystemcog.org/site_media/projects/esmf/pres_0812_board_gerhard.pdf, 2008

Valcke, S., 2013: The OASIS3 coupler: A European climate modelling community software. Geosci. Model Dev., 6, 373–388, doi:10.5194/gmd-6–373-2013

Valcke, S., Balaji, V., Craig, A., Deluca, C., Dunlap, R., Ford, R. W., Jacob, R., Larson, J., Okuinghttons, R., Riley, G., Vertenstein, M: Coupling technologies for Earth System Modelling, Geosci. Model Dev., 5, 1589-1596, 2012.

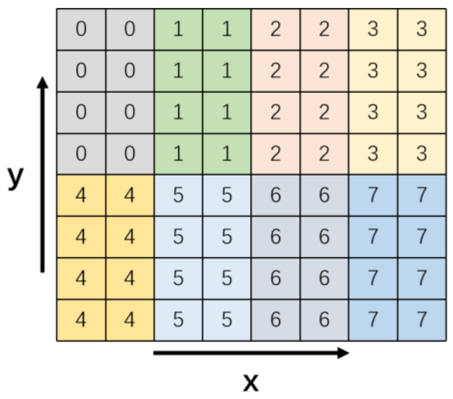

(a) A regular 2-D parallel decomposition in both X and Y direction

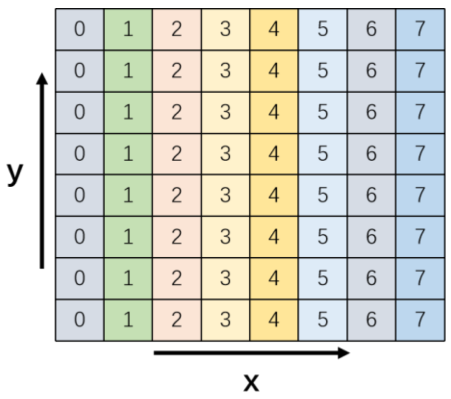

(b) A regular 1-D parallel decomposition in only X direction

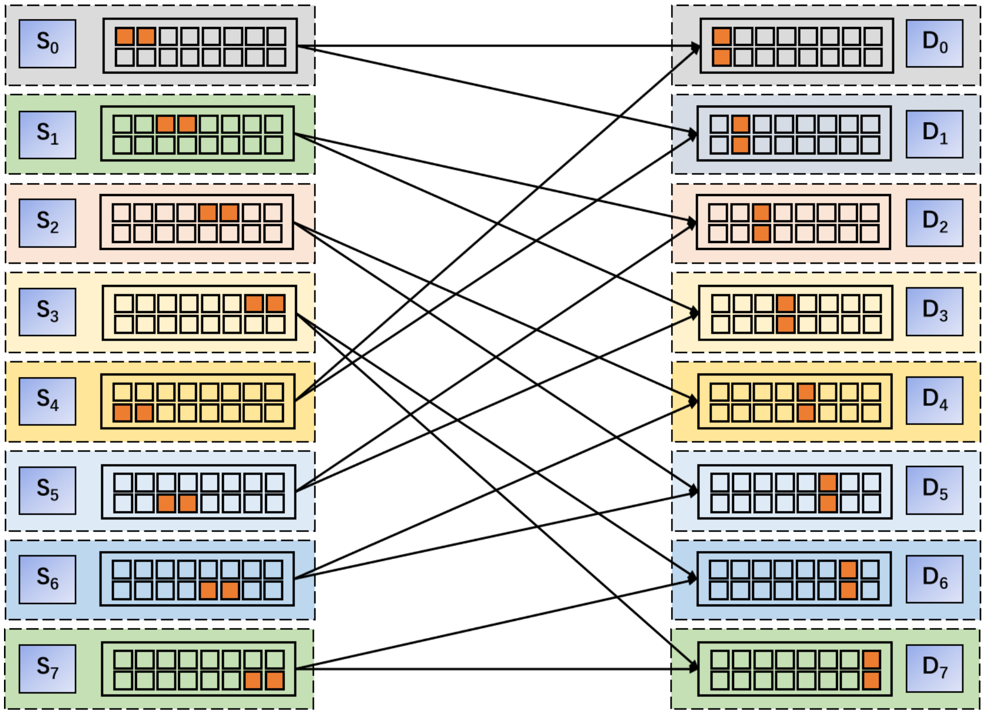

(c) The routing network from the parallel decomposition in Fig. 1a (**S**ource) to the parallel decomposition in Fig. 1(b) (**D**estination).

Figure 1. Two sample parallel decompositions of an 8x8 grid under 8 processes (Fig. 1a and 1b) and the routing network between them (Fig. 1c). Each colour corresponds to a process)

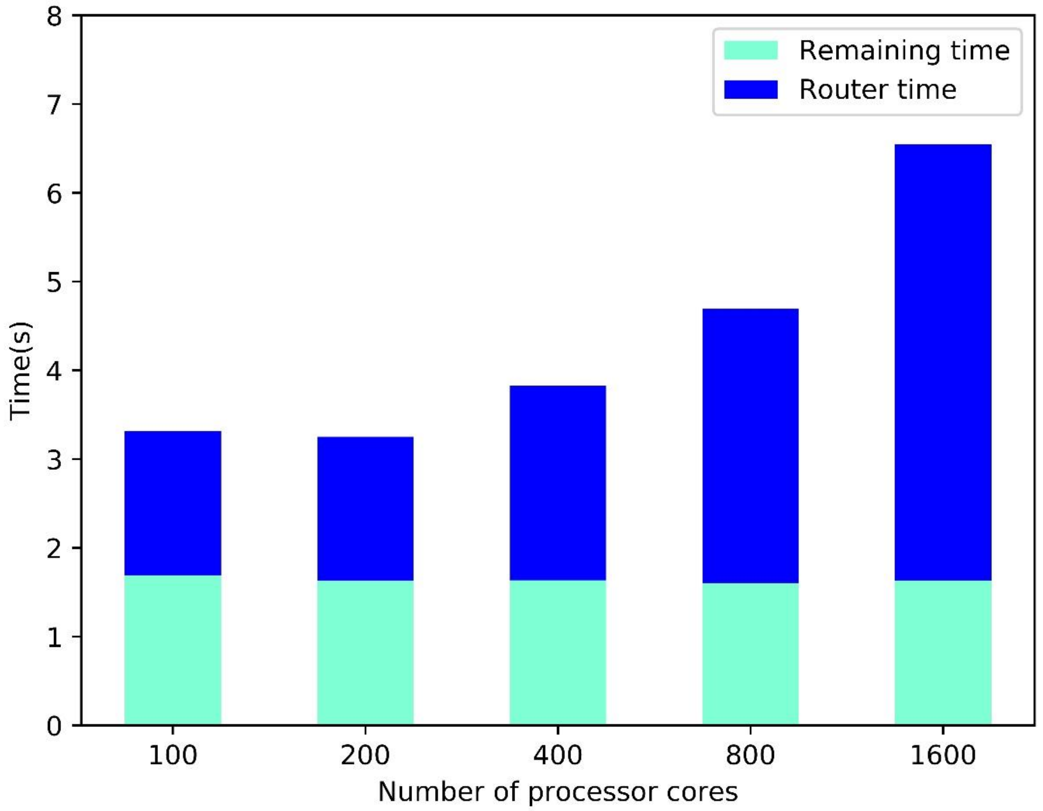

Figure 2. The total time of routing network generation (router time) and the remaining time for initializing a two-way MCT coupling between two toy component models. One toy component model uses a longitude-latitude grid with 4 million points and a regular 2-D parallel decomposition, while the other uses a cubed-sphere grid at 0.3 degree and a round-robin parallel decomposition. The time for reading an offline remapping weight file has been taken account in the remaining time, and a regular 1-D parallel decomposition is designed for the data interpolation. The supercomputer as well as the corresponding software stacks described in Section 4 is used for this test.

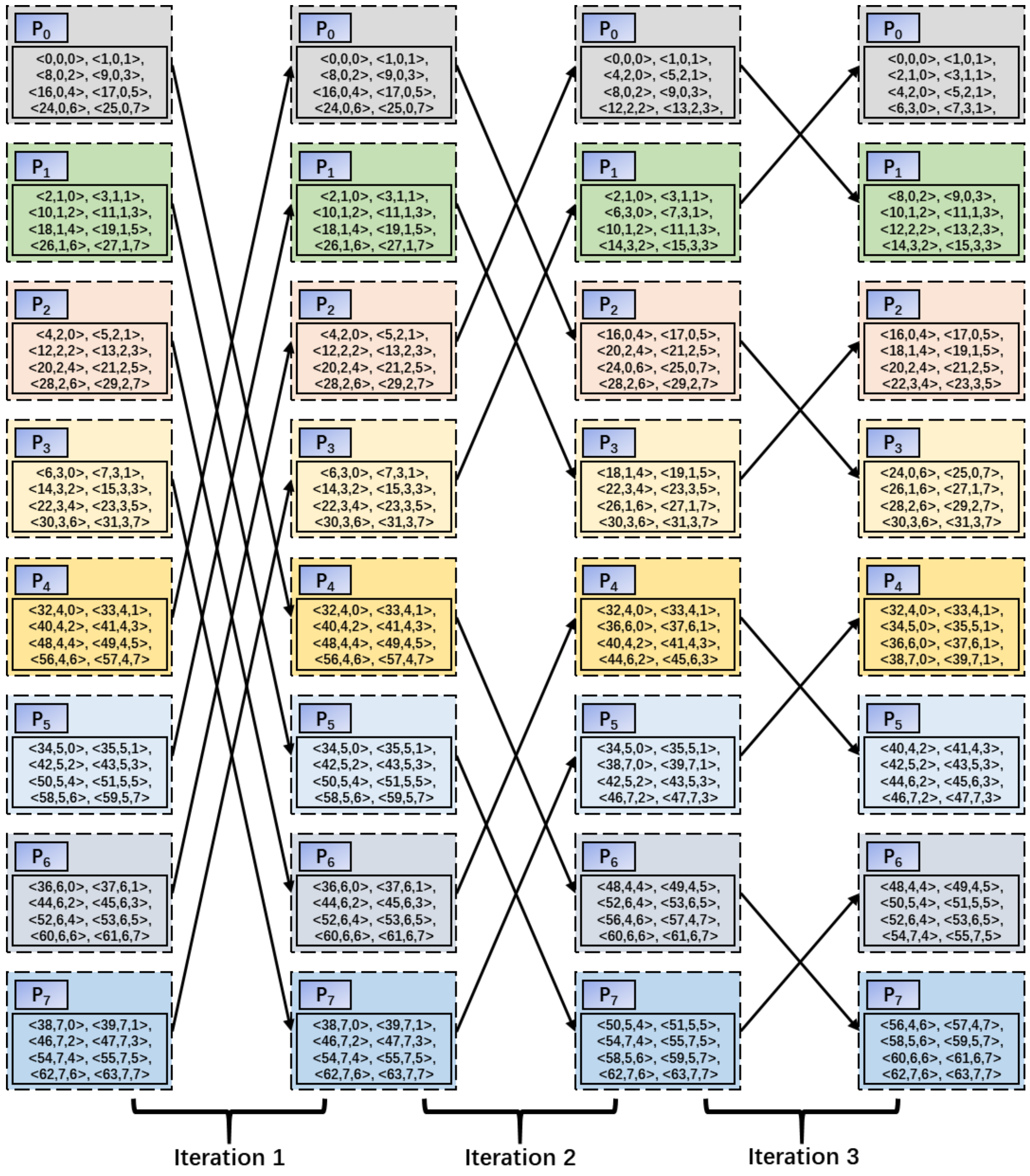

Figure 3. The distributed sort corresponding to the CLGMT entries in Table 1. Each iteration makes the CLGMT entries with larger global cell indexes reserved in the processes with larger IDs. For example, after the first iteration, the CLGMT entries with global cell indexes between 0 and 31 are reserved in P0~P3, while the remaining CLGMT entries are reserved in P4~P7.

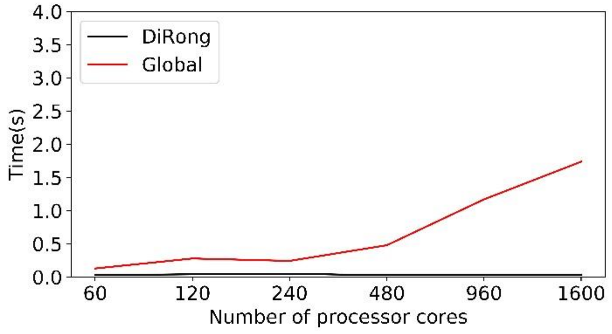

(a) The execution time of DiRong1.0 and the global under different core numbers and the grid size of 500,000.

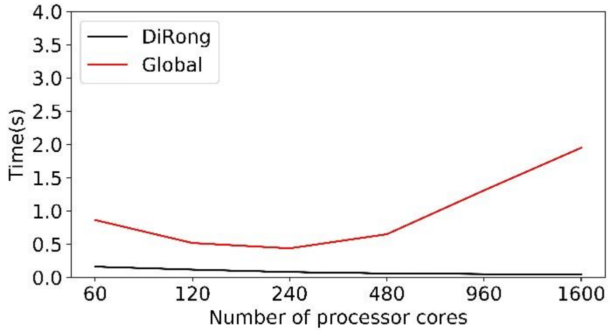

(b) The execution time of DiRong1.0 and the global under different core numbers and the grid size of 4,000,000.

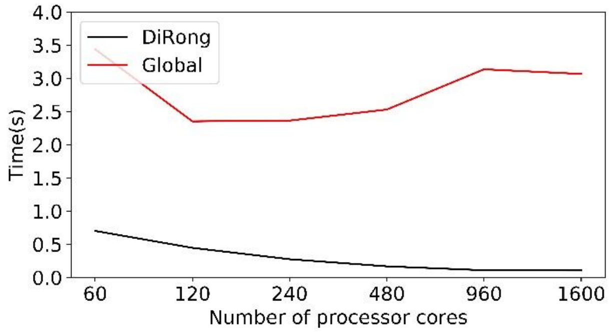

(c) The execution time of DiRong1.0 and the global under different core numbers and the grid size of 16,000,000.

Figure 4. Performance of DiRong1.0 and the comparison with the original global routing network generation (Global) under different core numbers and grid sizes. Two toy component models use the same number of processor cores in each test case. The comparison of the two algorithms in these figures shows that the acceleration effect of DiRong1.0 is more obvious when the number of grids and the number of processes is larger, that is, DiRong1.0 has higher parallel efficiency and better scalability.

Table 1. The Cell Local-Global Mapping Table (CLGMT) of the parallel decomposition in Fig. 1a

Process ID	Cell Local-Global Mapping Table entries
0	<0,0,0>, <1,0,1>, <8,0,2>, <9,0,3>, <16,0,4>, <17,0,5>, <24,0,6>, <25,0,7>
1	<2,1,0>, <3,1,1>, <10,1,2>, <11,1,3>, <18,1,4>, <19,1,5>, <26,1,6>, <27,1,7>
2	<4,2,0>, <5,2,1>, <12,2,2>, <13,2,3>, <20,2,4>, <21,2,5>, <28,2,6>, <29,2,7>
3	<6,3,0>, <7,3,1>, <14,3,2>, <15,3,3>, <22,3,4>, <23,3,5>, <30,3,6>, <31,3,7>
4	<32,4,0>, <33,4,1>, <40,4,2>, <41,4,3>, <48,4,4>, <49,4,5>, <56,4,6>, <57,4,7>
5	<34,5,0>, <35,5,1>, <42,5,2>, <43,5,3>, <50,5,4>, <51,5,5>, <58,5,6>, <59,5,7>
6	<36,6,0>, <37,6,1>, <44,6,2>, <45,6,3>, <52,6,4>, <53,6,5>, <60,6,6>, <61,6,7>
7	<38,7,0>, <39,7,1>, <46,7,2>, <47,7,3>, <54,7,4>, <55,7,5>, <62,7,6>, <63,7,7>

Table 2. The Cell Local-Global Mapping Table (CLGMT) of the parallel decomposition in Fig. 1b

Process ID	Cell Local-Global Mapping Table entries
0	<0,0,0>, <8,0,1>, <16,0,2>, <24,0,3>, <32,0,4>, <40,0,5>, <48,0,6>, <56,0,7>
1	<1,1,0>, <9,1,1>, <17,1,2>, <25,1,3>, <33,1,4>, <41,1,5>, <49,1,6>, <57,1,7>
2	<2,2,0>, <10,2,1>, <18,2,2>, <26,2,3>, <34,2,4>, <42,2,5>, <50,2,6>, <58,2,7>
3	<3,3,0>, <11,3,1>, <19,3,2>, <27,3,3>, <35,3,4>, <43,3,5>, <51,3,6>, <59,3,7>
4	<4,4,0>, <12,4,1>, <20,4,2>, <28,4,3>, <36,4,4>, <44,4,5>, <52,4,6>, <60,4,7>
5	<5,5,0>, <13,5,1>, <21,5,2>, <29,5,3>, <37,5,4>, <45,5,5>, <53,5,6>, <61,5,7>
6	<6,6,0>, <14,6,1>, <22,6,2>, <30,6,3>, <38,6,4>, <46,6,5>, <54,6,6>, <62,6,7>
7	<7,7,0>, <15,7,1>, <23,7,2>, <31,7,3>, <39,7,4>, <47,7,5>, <55,7,6>, <63,7,7>

Table 3. The distributed CLGMT after rearranging the CLGMT entries in Table 2

Process ID	**CLGMT entries**
0	<0,0,0>, <1,1,0>, <2,2,0>, <3,3,0>, <4,4,0>, <5,5,0>, <6,6,0>, <7,7,0>
1	<8,0,1>, <9,1,1>, <10,2,1>, <11,3,1>, <12,4,1>, <13,5,1>, <14,6,1>, <15,7,1>
2	<16,0,2>, <17,1,2>, <18,2,2>, <19,3,2>, <20,4,2>, <21,5,2>, <22,6,2>, <23,7,2>
3	<24,0,3>, <25,1,3>, <26,2,3>, <27,3,3>, <28,4,3>, <29,5,3>, <30,6,3>, <31,7,3>
4	<32,0,4>, <33,1,4>, <34,2,4>, <35,3,4>, <36,4,4>, <37,5,4>, <38,6,4>, <39,7,4>
5	<40,0,5>, <41,1,5>, <42,2,5>, <43,3,5>, <44,4,5>, <45,5,5>, <46,6,5>, <47,7,5>
6	<48,0,6>, <49,1,6>, <50,2,6>, <51,3,6>, <52,4,6>, <53,5,6>, <54,6,6>, <55,7,6>
7	<56,0,7>, <57,1,7>, <58,2,7>, <59,3,7>, <60,4,7>, <61,5,7>, <62,6,7>, <63,7,7>

Table 4. The Sharing Relationship Table (SRT) calculated from the rearranged distributed CLGMT entries in Fig. 3 and Table 3.

Process ID	Sharing Relationship Table entries
0	<0,0,0,0,0>, <1,0,1,1,0>, <2,1,0,2,0>, <3,1,1,3,0>, <4,2,0,4,0>, <5,2,1,5,0>, <6,3,0,6,0>, <7,3,1,7,0>
1	<8,0,2,0,1>, <9,0,3,1,1>, <10,1,2,2,1>, <11,1,3,3,1>, <12,2,2,4,1>, <13,2,3,5,1>, <14,3,2,6,1>, <15,3,3,7,1>
2	<16,0,4,0,2>, <17,0,5,1,2>, <18,1,4,2,2>, <19,1,5,3,2>, <20,2,4,4,2>, <21,2,5,5,2>, <22,3,4,6,2>, <23,3,5,7,2>
3	<24,0,6,0,3>, <25,0,7,1,3>, <26,1,6,2,3>, <27,1,7,3,3>, <28,2,6,4,3>, <29,2,7,5,3>, <30,3,6,6,3>, <31,3,7,7,3>
4	<32,4,0,0,4>, <33,4,1,1,4>, <34,5,0,2,4>, <35,5,1,3,4>, <36,6,0,4,4>, <37,6,1,5,4>, <38,7,0,6,4>, <39,7,1,7,4>
5	<40,4,2,0,5>, <41,4,3,1,5>, <42,5,2,2,5>, <43,5,3,3,5>, <44,6,2,4,5>, <45,6,3,5,5>, <46,7,2,6,5>, <47,7,3,7,5>
6	<48,4,4,0,6>, <49,4,5,1,6>, <50,5,4,2,6>, <51,5,5,3,6>, <52,6,4,4,6>, <53,6,5,5,6>, <54,7,4,6,6>, <55,7,5,7,6>
7	<56,4,6,0,7>, <57,4,7,1,7>, <58,5,6,2,7>, <59,5,7,3,7>, <60,6,6,4,7>, <61,6,7,5,7>, <62,7,6,6,7>, <63,7,7,7,7>

Table 5. The SRT entries distributed in the *src* component model after rearranging the SRT in Table 4

Process ID	Sharing Relationship Table entries
0	<0,0,0,0,0>, <1,0,1,1,0>, <8,0,2,0,1>, <9,0,3,1,1>, <16,0,4,0,2>, <17,0,5,1,2>, <24,0,6,0,3>, <25,0,7,1,3>
1	<2,1,0,2,0>, <3,1,1,3,0>, <10,1,2,2,1>, <11,1,3,3,1>, <18,1,4,2,2>, <19,1,5,3,2>, <26,1,6,2,3>, <27,1,7,3,3>
2	<4,2,0,4,0>, <5,2,1,5,0>, <12,2,2,4,1>, <13,2,3,5,1>, <20,2,4,4,2>, <21,2,5,5,2>, <28,2,6,4,3>, <29,2,7,5,3>
3	<6,3,0,6,0>, <7,3,1,7,0>, <14,3,2,6,1>, <15,3,3,7,1>, <22,3,4,6,2>, <23,3,5,7,2>, <30,3,6,6,3>, <31,3,7,7,3>
4	<32,4,0,0,4>, <33,4,1,1,4>, <40,4,2,0,5>, <41,4,3,1,5>, <48,4,4,0,6>, <49,4,5,1,6>, <56,4,6,0,7>, <57,4,7,1,7>
5	<34,5,0,2,4>, <35,5,1,3,4>, <42,5,2,2,5>, <43,5,3,3,5>, <50,5,4,2,6>, <51,5,5,3,6>, <58,5,6,2,7>, <59,5,7,3,7>
6	<36,6,0,4,4>, <37,6,1,5,4>, <44,6,2,4,5>, <45,6,3,5,5>, <52,6,4,4,6>, <53,6,5,5,6>, <60,6,6,4,7>, <61,6,7,5,7>
7	<38,7,0,6,4>, <39,7,1,7,4>, <46,7,2,6,5>, <47,7,3,7,5>, <54,7,4,6,6>, <55,7,5,7,6>, <62,7,6,6,7>, <63,7,7,7,7>

Table 6. The SRT entries distributed in the *dst* component model after rearranging the SRT in Table 4

Process ID	Sharing Relationship Table entries
0	<0,0,0,0,0>, <8,0,2,0,1>, <16,0,4,0,2>, <24,0,6,0,3>, <32,4,0,0,4>, <40,4,2,0,5>, <48,4,4,0,6>, <56,4,6,0,7>
1	<1,0,1,1,0>, <9,0,3,1,1>, <17,0,5,1,2>, <25,0,7,1,3>, <33,4,1,1,4>, <41,4,3,1,5>, <49,4,5,1,6>, <57,4,7,1,7>
2	<2,1,0,2,0>, <10,1,2,2,1>, <18,1,4,2,2>, <26,1,6,2,3>, <34,5,0,2,4>, <42,5,2,2,5>, <50,5,4,2,6>, <58,5,6,2,7>
3	<3,1,1,3,0>, <11,1,3,3,1>, <19,1,5,3,2>, <27,1,7,3,3>, <35,5,1,3,4>, <43,5,3,3,5>, <51,5,5,3,6>, <59,5,7,3,7>
4	<4,2,0,4,0>, <12,2,2,4,1>, <20,2,4,4,2>, <28,2,6,4,3>, <36,6,0,4,4>, <44,6,2,4,5>, <52,6,4,4,6>, <60,6,6,4,7>
5	<5,2,1,5,0>, <13,2,3,5,1>, <21,2,5,5,2>, <29,2,7,5,3>, <37,6,1,5,4>, <45,6,3,5,5>, <53,6,5,5,6>, <61,6,7,5,7>
6	<6,3,0,6,0>, <14,3,2,6,1>, <22,3,4,6,2>, <30,3,6,6,3>, <38,7,0,6,4>, <46,7,2,6,5>, <54,7,4,6,6>, <62,7,6,6,7>
7	<7,3,1,7,0>, <15,3,3,7,1>, <23,3,5,7,2>, <31,3,7,7,3>, <39,7,1,7,4>, <47,7,3,7,5>, <55,7,5,7,6>, <63,7,7,7,7>

Table 7. Performance of DiRong1.0 and the comparison with the original global routing network generation (Global) when concurrently increasing the grid size and core number.

Core number of each toy component model	**Grid size**	**Execution time (s) of DiRong1.0**	**Execution time (s) of Global**	**Global/DiRong1.0**
200	500,000	0.029	0.214	7.38
400	1,000,000	0.033	0.453	13.73
800	2,000,000	0.039	1.008	25.85
1600	4,000,000	0.045	1.949	43.31